Signal Processing Improvements for Smart Antenna Signals in IS-95 CDMA

Sofiène AFFES and Paul MERMELSTEIN

INRS-Télécommunications, Université du Québec
16, Place du Commerce, Ile des Soeurs, Verdun, QC, H3E 1H6, Canada
Tel: (1) (514) 765.7817/7769 - Fax: (1) (514) 761.8501
E-mail: affes,mermel@inrs-telecom.uquebec.ca

Abstract— **We propose an efficient signal processing technique to exploit smart antennas in IS-95 CDMA. It integrates decision feedback identification (DFI) and new decision variables into the adaptive antenna beamforming scheme. These two features permit implementation of a coherent detection on the uplink without a pilot and spatio-temporal maximum ratio combining (MRC). With two antennas and nonselective fading, the additional gain in SNR achieved by either feature is as significant as the gain obtained by simple antenna beamforming over diversity combining. Up to 2 dB performance advantage is obtained in selective fading as compared to simple beamforming.**

I. Introduction

Smart antennas promise to satisfy the challenging demand for capacity due to the huge amount of wireless data to be supported in the future. The current IS-95 air interface standard proposes the use of 3 sectorized antennas but does not specify any kind of array processing [1],[2]. Antennas may be used in a simple diversity combining scheme to achieve improvements in capacity [3]. However, simple beamforming, as proposed in [4], achieves better performance. Beamforming exploits multipath and space diversity as efficiently as diversity combining, however it achieves greater interference reduction and increased capacity. We show here that additional enhancements are still achievable with smart antennas by the integration of improved array signal processing with antenna beamforming.

Using STAR, a novel Subspace-Tracking Array-Receiver [5], we first replace the iterative eigen-decomposition in [4] by a very simple LMS-type eigen-subspace tracking procedure. This adaptive identification step shows faster convergence and tracking capabilities of the propagation vectors [5]. It also allows for the feedback of "forced" decisions over estimated symbols as commonly proposed in equalization. This new feature, denoted here by decision feedback identification (DFI), removes the phase ambiguity over estimated symbols. Compared to [4], it achieves a coherent detection gain of 3 dB in interference reduction on the uplink without a pilot. Therefore, it reduces the symbol error rate (SER) and results in a potential increase in capacity. It also permits the incorporation of a new decision variable that implements a spatio-temporal MRC combining with further improved results in SER and in capacity, especially in selective fading environments.

This work was supported by the Bell Quebec/Nortel/NSERC Industrial Research Chair in Personal Communications.

0-7803-4872-9/98/$10.00 © 1998 IEEE

Simulations in both selective and nonselective Rayleigh fading environments confirm the effectiveness of the proposed improvements and clearly show that STAR outperforms the antenna beamforming scheme proposed in [4].

II. Formulation and Background

A. Assumptions and Model

We consider a CDMA cellular system in which each base-station is equipped with M receiving antennas. We are particularly interested in the uplink, but we shall see that the proposed technique is applicable to the downlink as well with similar advantages.

We consider a multipath environment with P paths. We assume that the multipath time-delays are perfectly estimated and tracked. Time synchronization and tracking are addressed in [6] where an efficient transceiver scheme combining acquisition and reception is proposed.

In the present IS-95 standard, information bits are coded by a convolutional encoder, grouped into $\log_2(L)$ bits, then coded into Walsh symbols, say $w_n \in \{1, \ldots, L\}$. For each symbol, the corresponding orthogonal Walsh sequence of length L is further spread by a PN sequence before final transmission. For the sake of simplicity, we do not identify separately the in-phase and quadrature components, but consider transmission over a complex channel.

At reception, the signal vector received at the M antennas is fed to a set of L Walsh correlators as shown in Fig. 1. These correlators implicitly execute the acquisition and the tracking of each path component as mentioned earlier. They also involve the despreading and sampling of the data at the symbol rate. Each correlator outputs signal samples on P fingers that correspond to the P multipath components in a RAKE-like structure. Notice however that each finger is a $(M \times 1)$-dimensional vector denoted by $Z^i_{p,n}$ and referred to as the post-correlation vector.

It is reasonable to assume that time-variations in the propagation characteristics are slow compared to the symbol duration and can be ignored over such an interval (*i.e.*, Walsh sequence). Therefore, at symbol iteration number n, we can write the post-correlation vector of the ith Walsh correlator for the pth path $Z^i_{p,n}$ as follows:

$$Z^i_{p,n} = G_{p,n}\psi_n\varepsilon_{p,n}\delta^i_n + N^i_{p,n} = G_{p,n}s^i_{p,n} + N^i_{p,n}\ , \qquad (1)$$

where $G_{p,n}$ is the $(M \times 1)$-dimensional propagation vector over the pth path, whose norm is fixed for convenience

to $\sqrt{M}$ (more details about model adjustments are given in [5]). The propagation model includes the effects of Rayleigh fading over different antennas. This fading is assumed independent in the simulations below. The total received power ψ_n^2 contains the effects of shadowing, path-loss and power control. The power fractions $\varepsilon_{p,n}^2$ represent a normalized power distribution of the total received power ψ_n^2 over the P multipaths (*i.e.*, $\sum_{p=1}^{P} \varepsilon_{p,n}^2 = 1$). The contributions of both the in-cell and out-cell interference at each correlator, as well as the background noise and self-interference due to multipath, are reasonably modeled by an uncorrelated zero-mean Gaussian white noise vector $N_{p,n}^i$ (*i.e.*, $R_N = \sigma_N^2 I_M$). Finally, δ_n^i is the result at iteration n of correlating the received Walsh symbol w_n by the ith Walsh correlator. Due to the orthogonality of Walsh sequences, δ_n^i is equal to 1 if $i = w_n$ and 0 otherwise. Therefore, the signal component $s_{p,n}^i = \psi_n \varepsilon_{p,n} \delta_n^i$ is zero at the output of all the correlators except the one corresponding to the received Walsh symbol (*i.e.*, $s_{p,n}^{w_n} = \psi_n \varepsilon_{p,n}$).

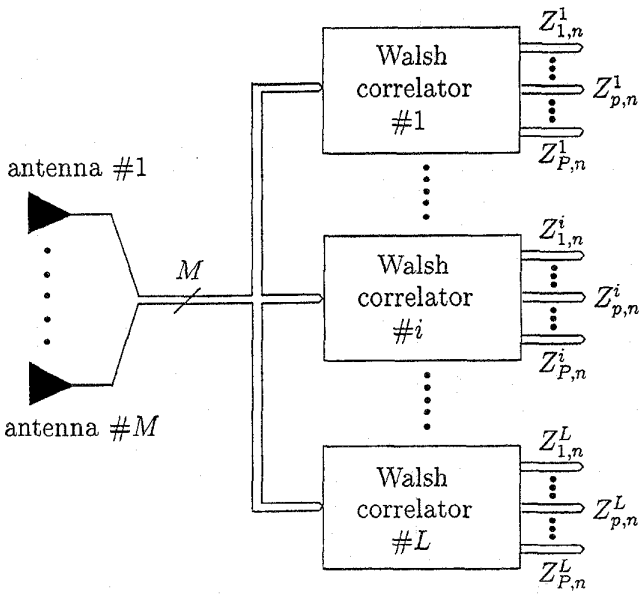

Fig. 1. Correlator structure at the base-station for a desired user: each branch implicitly involves baseband IQ demodulation, A/D conversion, acquisition and tracking of each path component as well as despreading and sampling of the data at the symbol rate. The M-dimensional vector $Z_{p,n}^i$ is the post-correlation vector of the ith Walsh correlator for the pth path at the symbol iteration number n.

B. Diversity Combining

With diversity combining, we simply sum at the output of each correlator all the powers collected over the different diversity paths (*i.e.*, spatio-temporal square law combining). The decision variable at the output of the ith Walsh correlator is then defined as follows:

$$d_n^i = \sum_{p=1}^{P} \|Z_{p,n}^i\|^2 / M \ , \qquad (2)$$

where the division by the number of antennas M is introduced for normalization. The L decision variables, each having an average value equal to $\psi_n^2 \delta_n^i + P\sigma_N^2$, are then fed to a soft decision Viterbi decoder.

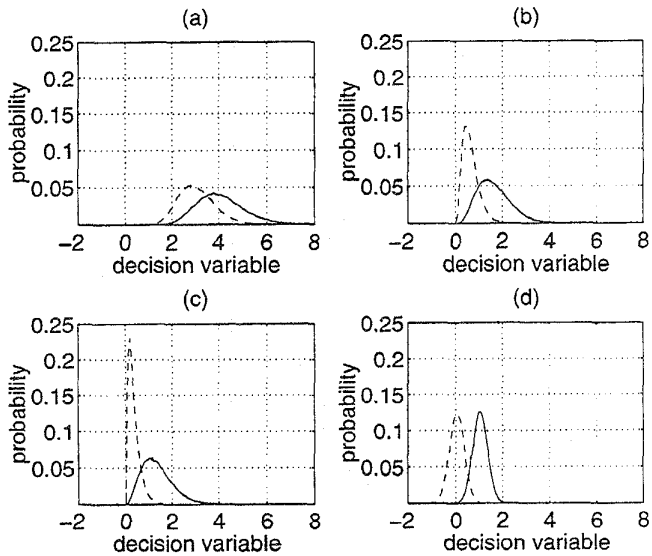

Fig. 2. Probability distribution function of the decision variable: correct decision (solid), wrong decision (dashed). (a): Diversity combining. (b): Simple antenna beamforming. (c): STAR with classical decision variable. (d): STAR with new decision variable. Configuration: $M = 5$ antennas, $P = 3$ paths with power distribution of 0, -3 and -6 dB, perfect power control (*i.e.*, $\psi_n^2 = 1$) and post-correlation $SNR = 0$ dB (*i.e.*, $\sigma_N^2 = 1$).

Fig. 2a shows the probability distribution functions of the decision variables d_n^i for the two cases, (i) when a correct correlator is used (*i.e.*, $i = w_n$) and (ii) when it is incorrect (*i.e.*, $i \neq w_n$). Intuitively, the overlap region under the two curves indicates the symbol error rate (SER) at the input of the soft decision Viterbi decoder, which in turn determines the bit error rate (BER) at its output.

For power control, we need timely estimates of the received symbols. Since the decision variables are decoded over relatively long symbol frames, we simultaneously estimate the received symbols by hard decision as follows:

$$\hat{w}_n = \underset{i \in \{1,\ldots,L\}}{\arg\max} \left\{ d_n^i \right\} \ . \qquad (3)$$

This immediate decision allows us to estimate the total received power $\hat{\psi}_n^2$ for power control by smoothing or averaging $d_n^{\hat{w}_n} - \sum_{i \neq \hat{w}_n} d_n^i / (L-1)$ over a given number of symbols [3].

Diversity combining efficiently exploits space diversity introduced by the antennas in addition to multipath diversity. The effect of fading in the total received power ψ_n^2 is indeed attenuated by averaging the fades over all multipaths and antennas. Therefore, the use of antennas in a simple diversity combining scheme reduces the time-variations of the total received power (or equivalently the average fading). This feature reduces the power control errors about the required received power and consequently improves the capacity [3].

However, diversity combining does not exploit the array processing capability of antennas to reduce interference. It simply sums the interference over all diversity branches. We show next that antenna beamforming further reduces interference by a factor M (*i.e.*, antenna gain) while it exploits space and multipath diversity in the same way as in diversity combining.

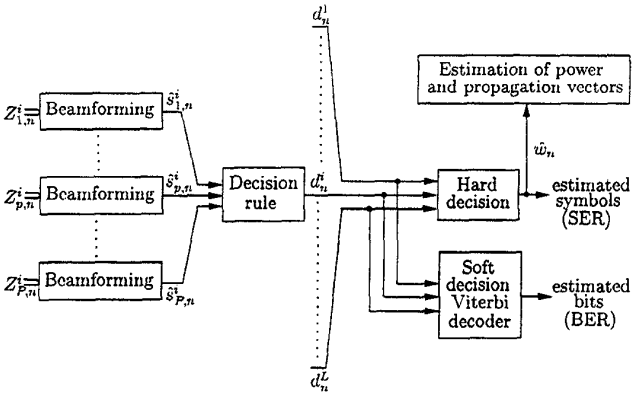

Fig. 3. Receiver structure at the base-station for a desired user: the beamforming of post-correlation vectors at each path and the combining of the resulting signal components in a decision variable are only shown at the ith Walsh correlator branch of Fig. 1.

C. Antenna Beamforming

As reference, we consider here a representative antenna beamforming method recently proposed by Naguib and Paulraj [4]. Assume that estimates of the propagation vectors are available at each iteration n within a phase ambiguity (*i.e.*, $\hat{G}_{p,n} \simeq e^{-j\phi_{p,n}} G_{p,n}$). This identification step will be explained soon below. At the output of each correlator (see Fig. 3), Naguib and Paulraj first estimate over each path the signal component $\hat{s}^i_{p,n}$ by matched beamforming (*i.e.*, spatial MRC combining) as follows:

$$\begin{aligned} \hat{s}^i_{p,n} &= \hat{G}^H_{p,n} Z^i_{p,n}/M \\ &\simeq e^{j\phi_{p,n}} \psi_n \varepsilon_{p,n} \delta^i_n + \hat{G}^H_{p,n} N^i_{p,n}/M \\ &\simeq e^{j\phi_{p,n}} s^i_{p,n} + \eta^i_{p,n} \ , \end{aligned} \tag{4}$$

where the residual interference $\eta^i_{p,n}$ has an average variance of σ^2_N/M. In this way, Naguib and Paulraj implement the antenna gain and reduce the level of interference by a factor M at the beamformer output. Since each signal component is estimated with a phase ambiguity, they next perform a temporal square law combining of these estimates and define the decision variables at the output of the Walsh correlators as follows:

$$d^i_n = \sum_{p=1}^{P} \left| \hat{s}^i_{p,n} \right|^2 \ . \tag{5}$$

These L values, which are on average equal to $\psi^2_n \delta^i_n + P\sigma^2_N/M$, are finally fed to a soft decision Viterbi decoder.

As shown intuitively in Fig. 2b, antenna beamforming reduces the symbol error rate that is indicated by the overlap region under the two curves, and therefore significantly increases the capacity. Due to a better reduction of interference, it also improves the estimation of received power for power control after hard decision as in Eq. (3).

As mentioned earlier, estimates of propagation vectors are required to achieve this beamforming scheme. Using the fact that the interference vector in Eq. (1) is an uncorrelated white noise vector, the identification of the propagation vector over each path $G_{p,n}$ can be simplified from [4] to characterize it as the principal eigenvector of the following matrix:

$$R_{Z_p} = E\left[Z^{w_n}_{p,n} Z^{w_n\,H}_{p,n} \right] = \psi^2 \varepsilon^2_p G_p G^H_p + \sigma^2_N I_M \ .$$

This is the correlation matrix over each path of the received post-correlation vector $Z^{w_n}_{p,n}$ resulting from the transmitted symbol w_n. Each vector $G_{p,n}$ is then estimated separately within an unknown phase ambiguity by an eigendecomposition of the sample correlation matrix $\hat{R}_{Z_p}$. This sample matrix can be easily obtained by averaging or smoothing the $Z^{\hat{w}_n}_{p,n}$ selected by hard decision using Eq. (3).

The antenna beamforming technique proposed by Naguib and Paulraj [4] efficiently implements the array processing gain and introduces a significant improvement in capacity. We show next that additional enhancements remain achievable.

III. The Proposed Structure: STAR

Assume first that estimates of the propagation vectors $\hat{G}_{p,n}$ are available at each iteration n as in the previous case of simple antenna beamforming. One key feature, as explained below is the identification of these vectors *without phase ambiguities*, contrary to [4] (*i.e.*, $\hat{G}_{p,n} \simeq e^{-j\phi_{p,n}} G_{p,n}$ where $\phi_{p,n} \simeq 0$). To this end, we apply matched beamforming like Naguib and Paulraj [4], but further take the real part of the beamformer output at each correlator as follows (see Fig. 3):

$$\begin{aligned} \hat{s}^i_{p,n} &= \Re e\left\{ \hat{G}^H_{p,n} Z^i_{p,n}/M \right\} \\ &\simeq \Re e\left\{ e^{j\phi_{p,n}} \right\} \psi_n \varepsilon_{p,n} \delta^i_n + \Re e\left\{ \hat{G}^H_{p,n} N^i_{p,n}/M \right\} \\ &\simeq s^i_{p,n} + \Re e\left\{ \eta^i_{p,n} \right\} \ . \end{aligned} \tag{6}$$

As a result, the variance of the residual interference $\Re e\left\{\eta^i_{p,n}\right\}$ is reduced by half relative to [4], down to $\sigma^2_{\text{res}} = \sigma^2_N/2M$ without distorting the signal component. This additional 3 dB gain is usually obtained in a coherent detection scheme after the recovery of the phase offset from the pilot on the downlink. So far, it has not been implemented on the uplink. This 3 dB coherent detection gain is achieved here by avoiding phase ambiguities without a pilot signal as explained shortly below.

Notice first that using Eq. (5), we can feed the L resulting decision variables d^i_n to a soft decision Viterbi decoder (see Fig. 3). Here, the decision variables have an average

power of $\psi_n^2\delta_n^i + P\sigma_N^2/2M$. Fig. 2c indicates the reduced symbol error rate at the decoder input and potential improvements in capacity and in power control compared to [4].

Instead of the classical definition of Eq. (5), we now consider new decision variables given by a weighted combination of the signal components (see Fig. 3):

$$d_n^i = \sum_{p=1}^{P} \hat{\varepsilon}_{p,n}\hat{s}_{p,n}^i \ , \tag{7}$$

where the squares of the weighting coefficients $\hat{\varepsilon}_{p,n}^2$ are the estimates of the normalized power fractions $\varepsilon_{p,n}^2$. These estimates are computed as follows:

$$\hat{\varepsilon}_{p,n}^2 = \frac{\xi_{p,n}^2}{\hat{\psi}_n^2} \ . \tag{8}$$

In Eq. (8), the estimate of the total received power $\hat{\psi}_n^2$ is given by:

$$\hat{\psi}_n^2 = \sum_{p=1}^{P} \xi_{p,n}^2 \ , \tag{9}$$

and allows for power control (see [5],[6]). On the other hand, the quantities $\xi_{p,n}^2$ which estimate here the amount of power received over each path $\psi_n^2\varepsilon_{p,n}^2$ are updated after hard decision of Eq. (3) by simple smoothing as follows:

$$\xi_{p,n+1}^2 = (1-\alpha)\xi_{p,n}^2 + \alpha \max\left\{ \left|\hat{s}_{p,n}^{\hat{w}_n}\right|^2 - \hat{\sigma}_{\text{res}}^2, 0 \right\}, \tag{10}$$

$$\hat{\sigma}_{\text{res}}^2 = (1-\alpha)\ \hat{\sigma}_{\text{res}}^2 + \alpha\ \frac{\sum_{i\neq\hat{w}_n}(d_n^i)^2}{L-1} \ , \tag{11}$$

where α is a smoothing factor, and where $\hat{\sigma}_{\text{res}}^2$ is a smoothed estimate of the variance of the residual interference after beamforming (see below Eq. (6)).

Contrary to Eq. (5) where the squared magnitudes are added to avoid phase ambiguities, the signal components are weighted in Eq. (7) by their respective normalized magnitudes (*i.e.*, notice that $\sum_{p=1}^{P}\hat{\varepsilon}_{p,n}^2 = 1$) before summation. This multipath matched-beamforming scheme implements a temporal MRC combining. Thus, the two consecutive spatial and multipath beamforming steps used to derive the new decision variables implement overall an optimal spatio-temporal MRC combining[1].

Notice that while the power of residual interference is accumulated over all paths and multiplied by P in Eq. (5), it is maintained in Eq. (7) at the same level[2] for all individual paths regardless of their number. This additional interference reduction, that we may call here *multipath gain* (by analogy to the antenna gain M), provides STAR a certain robustness to selective fading, as confirmed below by simulations. Additionally, the new decision variables, which are on average equal to $\psi_n\delta_n^i$, are not limited to positive values and allow the distributions to be better separated. As shown in Fig. 2d, the overlap region of the two distributions is further reduced, improving the resulting symbol error rate at the input of the soft decision Viterbi decoder and resulting in additional improvements in capacity and in power control.

As mentioned earlier, the above results rely on the identification of propagation vectors $G_{p,n}$ without phase ambiguities. To do so, we propose a simple and fast LMS-type eigen-subspace tracking procedure [5],[6] given by:

$$\hat{G}_{p,n+1} = \hat{G}_{p,n} + \mu_{p,n}\left(Z_{p,n}^{\hat{w}_n} - \hat{G}_{p,n}\widehat{s_{p,n}^{w_n}}\right)\widehat{s_{p,n}^{w_n}} \ , \tag{12}$$

where $\mu_{p,n}$ is an adaptation step-size, possibly normalized, and where the reference signal $\widehat{s_{p,n}^{w_n}} = \xi_{p,n} = \hat{\psi}_n\hat{\varepsilon}_{p,n}$ is actually the signal component estimate forced to be real and positive (not to be confused with $\hat{s}_{p,n}^{\hat{w}_n}$).

Other eigen-subspace tracking techniques are not excluded *a priori*. However, what it is original about the adaptive identification procedure we propose is that it includes decision feedback through the estimates of the signal components $\widehat{s_{p,n}^{w_n}}$. Without this feature (*i.e.*, in Eq. (12), using $\hat{s}_{p,n}^{\hat{w}_n}$ of Eq. (4) with the decision variables of Eq. (5) instead of $\widehat{s_{p,n}^{w_n}}$), the estimated propagation vectors $\hat{G}_{p,n}$ would converge to $G_{p,n}$ within an unknown phase ambiguity as in [4]. This ambiguity would also rotate the constellation of the estimated signal component (*i.e.*, $\psi_n\varepsilon_{p,n}e^{j\phi_{p,n}}$, see Eq. (4)). We see this rotation as a degree of freedom that allows for the incorporation of an additional constraint on the required position of the signal constellation (*i.e.*, $\psi_n\varepsilon_{p,n}$). Therefore, assigning $\widehat{s_{p,n}^{w_n}}$ to be real and positive by Eq. (6) and Eq. (10) respectively and feeding it back in the tracking equation (12) as a reference signal removes the ambiguity by preventing this rotation and forces all the phases $\phi_{p,n}$ to 0. We refer to this adaptive process as decision feedback identification (DFI). Through coherent detection and MRC combining, it allows for significant improvements in capacity and in power control as mentioned above and as verified below by simulations.

The convergence of $\hat{G}_{p,n}$ to $G_{p,n}$ without ambiguity is made possible by the flexibility of the adaptive identification of Eq. (12), which enables the integration of decision feedback. Other eigen-subspace methods such as the eigen-decomposition proposed by Naguib and Paulraj [4] identify propagation vectors with phase ambiguities, but usually have no control over them and/or do not incorporate decision feedback, leading to poorer performance. In addition, it should be noted that eigen-decomposition introduces a memory effect in the estimation of the sample matrix which is undesirable when tracking rapidly changing channels. On the other hand, LMS-type adaptive eigen-subspace tracking yields better tracking of propagation vectors in the presence of strong nonstationarities and is capable of adapting to high variations in received power [5].

Notice finally that the interference reduction achieved by the extraction of the real part in Eq. (6) can be obtained

[1]Spatio-temporal MRC combining could be implemented in one step as done in [6] in a different context.

[2]This explains the fact that we estimate σ_{res}^2 in Eq. (11) by smoothing an average power of the decision variables over the wrong symbols; to subtract it later as a bias in Eq. (10).

with DBPSK signaling as well [5]. Also, the resulting gain in SNR is still achievable in the case of $M = 1$ antenna. Hence, an application of STAR to the downlink could be viewed with the same potential enhancements. This issue is presently under study.

IV. Simulation Results

We compare in this section the performance in SER obtained by hard decision at the input of the soft decision Viterbi decoder with the post-correlation SNR. The results are given for diversity combining, simple antenna beamforming, STAR with the classical decision variables of Eq. (5) and STAR with the new decision variables of Eq. (7). The decision variables for the first three cases are simply estimated in parallel from the data processed by STAR with the new decision variables of Eq. (7). Therefore, they do not include the effects of errors in identification and/or power control errors that may result when these variables are fed back to separate processes. Hence, for all but the last case the resulting SER values are slightly optimistic.

The evaluations consider voice calls at a data rate of 9.6 kb/s spread over a 1.25 MHz band using a processing gain of 128. We use 2 antennas and assume a slow Rayleigh fading channel with a Doppler frequency shift of $f_D \simeq 2$ Hz simulated by Jakes' model [7]. We also assume that the data has been coded by a convolutional encoder at the rate 1/3 and mapped into 64-ary Walsh symbols at the rate of 4.8 kb/s before interleaving with a 32×6 matrix. We finally introduce a 10% error over the power control bit which is transmitted every 1.25 ms (*i.e.*, duration of 6 symbols) with a delay of 1.25 ms. This bit indicates to the mobile to either increase or decrease its power by a constant step-size of 0.5 dB.

In Fig. 4, we first consider a nonselective fading environment (*i.e.*, $P = 1$ path). Simulation results of Fig. 4a clearly indicate that the gain in SNR achieved by STAR with the classical decision variables (dotted) over simple antenna beamforming (semi-dashed) is as significant as the gain achieved by antenna beamforming over diversity combining (dashed) using 2 antennas. They hence confirm the additional improvement due to the single contribution of the proposed decision feedback identification (DFI) feature in the beamforming scheme. This feature implements a coherent detection gain of 3 dB without a pilot. Besides, simulation results show that the gain in SNR achieved by the new decision variables over the classical ones is of the same order. Hence, they also demonstrate the efficiency of the new decision variables which implement an optimal spatio-temporal MRC combining. The curves obtained from the theoretical situation of perfect power control and identification in Fig. 4b validate the simulation results. They indicate a slight degradation in Fig. 4a due to imperfect power control and identification errors, which becomes more noticeable at lower SNR values.

We next consider a selective fading environment with $P = 3$ paths as shown in Fig. 5. Simulation results of Fig. 5a again confirm the improvement due to DFI (dotted) relative to simple antenna beamforming (semi-dashed), as

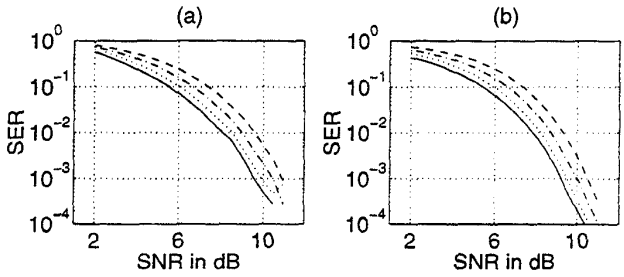

Fig. 4. SER versus post-correlation SNR per symbol: diversity combining (dashed), simple antenna beamforming (semi-dashed), STAR with classical decision variable(dotted), STAR with new decision variable (solid). (a): Simulations. (b): Perfect power control and identification. Configuration: $M = 2$ antennas, $P = 1$ path.

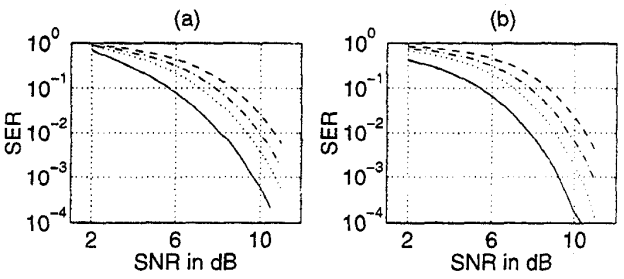

Fig. 5. SER versus post-correlation SNR per symbol (see caption of Fig. 4). Configuration: $M = 2$ antennas, $P = 3$ paths with equal power distribution.

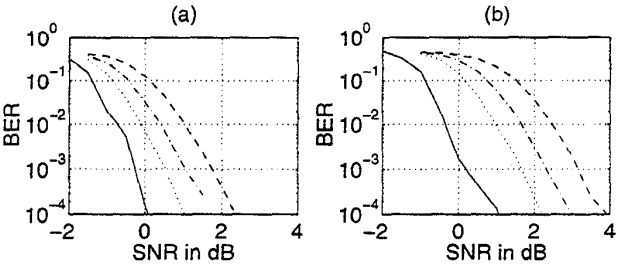

Fig. 6. BER obtained by simulations after soft decision Viterbi decoding versus post-correlation SNR per bit (see caption of Fig. 4). (a): nonselective fading configuration of Fig. 4. (b): selective fading configuration of Fig. 5.

well as the additional enhancement due to the new decision variables (solid). These results are again validated by the theoretical curves of Fig. 5b. More importantly, what we notice from this set of experiments in selective fading is that the gain obtained with the new decision variables over the classical ones is more significant in the presence of multipath, theoretically as well as by simulations. Compared to the nonselective fading results of Fig. 4, the performance of the new decision variables remain unchanged (see solid line curves), while those of the classical decision variables degrade regardless of the combining scheme (see other curves). This confirms the robustness of the new decision variables to multipath, due to the multipath gain of the temporal MRC combining step mentioned above in section III.

Finally, we give in Fig. 6 the BER computed by simulations after soft decision Viterbi decoding in both the nonselective and selective fading situations. For each method it shows the range of required SNR from which the capacity can be derived at a given BER following the methodology given in [3].

V. Conclusion

The proposed IS-95 CDMA compatible subspace-tracking array-receiver (STAR) employs simple eigen-subspace tracking and integrates decision feedback identification (DFI) and new decision variables. DFI implements a coherent detection gain of 3 dB in interference reduction without a pilot, while the new decision variables reduce SER and implement a multipath gain and robustness to selective fading by an optimal spatio-temporal MRC combining. At a required SER of 10^{-2}, DFI and the new decision variables each achieve an additional improvement in SNR (*i.e.*, capacity) as significant as the gain achieved by simple antenna beamforming over diversity combining with 2 antennas and nonselective fading. These enhancements become even more significant in selective fading where a 2 dB advantage over simple antenna beamforming is realized at a SER of 10^{-2} by DFI and the new decision variables. Compared to diversity combining, even greater gains are achievable with more antennas. Finally, STAR provides fast channel tracking and efficient power control, and requires a low complexity of $O(MP)$ per correlator branch.

References

[1] *An Overview of the Application of Code Division Multiple Access (CDMA) to Digital Cellular Systems and Personal Cellular Networks*, Qualcomm, Inc., USA, 1992.

[2] A.J. Viterbi, *CDMA Principles of Spread Spectrum Communication*, Addison-Wesley, 1995.

[3] A. Jalali and P. Mermelstein, "Effects of diversity, power control, and bandwidth on the capacity of microcellular CDMA systems", *IEEE Journal on Selected Areas in Communications*, vol. 12, pp. 952-961, June 1994.

[4] A.F. Naguib and A. Paulraj, "Performance of wireless CDMA with M-ary orthogonal modulation and cell site antenna arrays", *IEEE Journal on Selected Areas in Communications*, vol. 14, pp. 1770-1783, December 1996.

[5] S. Affes and P. Mermelstein, "Capacity improvement of cellular CDMA by the subspace-tracking array-receiver", *Proc. of IEEE Signal Processing Workshop on Signal Processing Advances in Wireless Communications SPAWC'97*, Paris, France, pp. 233-236, April 16-18, 1997.

[6] S. Affes and P. Mermelstein, "A new receiver structure for asynchronous CDMA: STAR - the spatio-temporal array-receiver", *IEEE Journal on Selected Areas in Communications*, accepted for publication in March 1998, to appear.

[7] W.C. Jakes, Ed., *Microwave Mobile Communications*, John Wiley & Sons, 1974.